Foo, SE., Tan, CM., & Beach, MA. (2003). Spatial temporal characterization of UTRA FDD channels at the user equipment. *IEEE 57th Vehicular Technology Conference, 2003 (VTC 2003-Spring)*, *2*, 793 - 797. https://doi.org/10.1109/VETECS.2003.1207734

Spatial Temporal Characterization of UTRA FDD Channels at the User Equipment

S. E. Foo, C. M. Tan and M. A. Beach
Centre for Communications Research
University of Bristol
Queens Building, University Walk, Clifton, Bristol BS8 1TR, United Kingdom.
E-mail: {s.e.foo, chor.min.tan, m.a.beach}@bris.ac.uk

***Abstract*— A directional channel sounding trial from the mobile terminal was recently performed in the city of Bristol. The trial provided temporal and full azimuth view of both channels in the UMTS[1] Terrestrial Radio Access (UTRA) Frequency Division Duplex (FDD) bands simultaneously via the use of a Uniform Circular Patch Array (UCPA). Extraction of the multipath components (MPC's) parameter was performed via a newly developed 2D Hybrid-Space Space-Alternating Generalized Expectation-Maximization (HS-SAGE) algorithm. Typical propagation mechanisms observed are described as seen from the respective sample Azimuth-Delay Power Spectrum (ADPS). The similarity of both duplex channels are verified. In addition, second order statistics of delay and azimuth parameters are presented where large azimuth spreads independent of mobile terminal orientation were observed.**

I. Introduction

Spatial processing, in addition to existing temporal processing, promises to provide increased performance and capacity gains crucial to meet the ever increasing demand for higher spectrum efficiency in wireless systems. This is evident in the current actively researched areas of Multiple-Input Multiple-Output (MIMO) systems and Smart Antennas. However, to provide a representative evaluation of such systems, accurate channel information that reflects the true environment envisaged for such applications is important.

In a typical macrocell scenario, directional information at the base station has been extensively measured and modelled [1][2][3]. However, little is mentioned of measurements from the mobile terminal in the literature. A channel sounding trial has been recently performed in the city of Bristol (UK) to provide a view of the UTRA FDD channel from the mobile terminal.

To address the well known issue in FDD systems of exploiting the information gained from the reception channels in a uncorrelated transmission channel, several authors have suggested that the delay and azimuth parameters of MPC's are similar for both channels [4][5]. This is especially crucial in systems exploiting spatial domain processing. Thus, knowledge of the reception channel can be utilized for transmission provided this is done within the coherence time and the duplex separation is not excessively large (approximately 10% for the UTRA FDD case).

[1]Universal Mobile Telecommunications System

Here, we are interested to verify the likeness of the duplex channels from a delay and azimuth statistical perspective. Naturally, the path coefficients would differ in an uncorrelated manner since they are subject to random superposition of unresolvable paths (due to limited resolution).

A Medav RUSK vector channel sounder was customized and deployed to sample the channel at 1910-1930MHz and 2110-2130MHz. A custom 8–element UCPA was designed and built to provide a 360° azimuth view of the environment.

This paper describes the measurement campaign, presents samples of the ADPS obtained via the newly developed 2D HS-SAGE algorithm, and analysis performed. In particular, emphasis is given to the distribution of second order statistics of the azimuth and delay parameters as seen in both channels.

II. Measurements

The Medav RUSK BRI vector channel sounder [8] was the basis of the equipment employed during the measurement trials. It operates on the principle of a periodic multi tone test signal, and measures the complex frequency response of the channel through each receiving array element via rapid multiplexing. Customizations were performed to enable sequential sampling of the channels centered at 1.92GHz and 2.12GHz, each with a bandwidth of 20MHz and a multi tone period of 6.4μs.

To enhance the signal to noise ratio, 8 snapshots, each consisting of the 8 complex frequency response measured from each antenna element, were rapidly recorded within approximately 1.6ms for each frequency band channel. For convenience, we call these octets of snapshots, Fast Doppler Blocks (FDB's). A rest period of about 22.5ms is inserted before the next FDB is measured. The 'mobile terminal' vehicle was driven at a predetermined speed such that these FDB's are spaced by $\frac{\lambda}{4}$ apart at 1.92GHz. Furthermore, a total of 246 FDB's were collected for each measurement spot with the vehicle driven at the constant speed of 5km/h. Therefore, each measurement location consists of data collected over approximately 62λ. This was done in an effort to obtain a more statistically robust ensemble of data for each location, and thus a more representative view of the channel characteristics with reduced spatial fading.

As mentioned, the measurements were performed in the city of Bristol. The urban environment is typical of a European city

Fig. 1. 'Mobile' Electric Car loaded with Receiver Equipment

with buildings of 2–3 storeys. A total of 62 measurements were performed in this scenario. The measurements were performed during working days to include typical variations in the channel as seen in a city.

The base station was located at the roof of the Physics Building (University of Bristol) and a commercially available UMTS panel antenna was employed with a corresponding base station antenna height of approximately 33m above ground. The furthest distance between the measurement locations and base station recorded was about 1.5km.

At the mobile end, a custom 8–element UCPA was designed and constructed as previously mentioned. The requirement for a full 360° azimuthal view led to the choice of a circular array over conventional uniform linear arrays (ULA)[6]. The patches provided good response over the frequency bands of interest [9] and the array was mounted at the rear of the mobile vehicle. An electric car (see Figure 1)was employed as it had a low roofline and was of glass reinforced plastic (GRP) construction, thus reducing undesirable effects of beampattern perturbation with metallic structures. The array was mounted such that it was just high enough to have a completely unobstructed view in the azimuth plane but low enough to provide the view of the typical channel seen by a pedestrian holding a mobile terminal at ear level. This compromise led to an equivalent height from ground level of the patches of approximately 1.8m, corresponding to a rather tall pedestrian.

A back to back calibration was meticulously performed at the start of each trial day to remove the response of the measurement equipment and to synchronize the rubidium reference clocks at the transmitter and receiver. This in turn ensured accurate phase relationship and time of flight.

III. Post Processing

The objective of post processing the collected complex frequency responses of the channels was to extract the delay, azimuth and path coefficient parameters of the MPC's. Super resolution techniques were employed to improve the inherent resolution limitations of the measurement hardware, although it has to be noted that the extend to which this can be accomplished is not unlimited.

The requirement for a full 360° azimuthal view at the mobile user led to the choice of an UCPA as mentioned above. From our previous evaluation, we found that SAGE offered the best performance in terms of accuracy for an 8–element UCPA [6]. Therefore, we decided to employ the SAGE algorithm. However, the iterative nature of SAGE places a significant burden on computational effort. In an attempt to alleviate this, the 2D HS-SAGE was developed and applied here in the frequency domain. For the MPC's, their Directions of Arrival (DoA) were extracted in the element-space [10], while their Time Delays of Arrival (TDoA) were extracted in the beamspace domain [7] thus the naming convention of HS-SAGE: joint element-space and beamspace processing. Briefly, the reduction in computational effort was afforded by the reduction of the size of the raw data by selectively forming beams in the delay domain only where significant energy exists.

In our case, we set a threshold of 30dB from the most powerful peak in the impulse response. For example, it was observed that most resultant impulse responses only had energy within this threshold over a span of approximately $2\mu s$. Therefore, rather than iterate in fine graticule over the entire excess delay of 6.4μs, the estimation is only performed within the region of significant energy by forming consecutive beams in this area. This reduces the size of the raw data and the span of the search iterations. As a consequence, significant reduction in computation time was achieved without sensibly sacrificing accuracy.

The 30dB cutoff threshold was used in the pre-processing scan of the impulse response as a 25dB noise rejection threshold was subsequently used in the estimation step. We found that within a threshold of 25dB, reliable identification of MPC's was possible in a separate test performed in the anechoic chamber with the equipment setup. In other words, MPC's with path coefficient 25dB weaker that the most powerful component were rejected as noise.

To obtain more robust samples of the channel, we averaged 2 FDB's and fed the resultant 8 by 129 complex frequency response matrix to be processed by the 2D HS-SAGE where 8 corresponds to the number of receive elements and 129 corresponds to the number of frequency samples that span 20MHz within an excess delay of 6.4μs. This results in MPC estimates for every $\frac{\lambda}{2}$ over the 61.5λ measured for each location, yielding 123 sets of MPC parameters per location. The smallest quantization grid size of the maximization step used was 0.5° in the azimuth domain and 5ns in the delay domain.

The 0.5° azimuth grid size corresponds to the angular step size used whilst performing the array manifold measurement in the anechoic chamber. The actual array manifolds were measured for both frequency bands and subsequently used in the correlation process of the 2D HS-SAGE to enhance the accuracy of the estimation. A maximum limit of 40 MPC's were estimated during each iteration based on the Successive Interference Cancellation (SIC) technique [7].

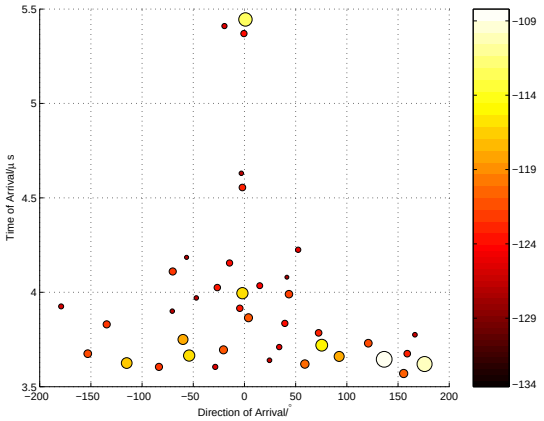

Fig. 2. Sample MPC's at 1.9GHz Band

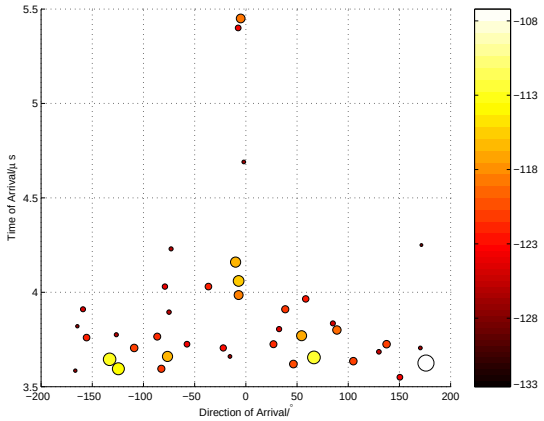

Fig. 3. Sample MPC's at 2.1GHz Band

IV. Results

A. View of Multipath Components

A sample of the MPC's estimated from one of the locations in the 1.9GHz channel is visualized in Figure 2. The size and shade of each circle represent the strength of the particular component. A lighter and bigger circle corresponds to a more powerful path, and vice-versa. It can be seen that the two dominant propagation mechanism here is local scattering and street canyon coupling.

The spread of components in the azimuth plane within the delay region of 3.6μs–3.8μs can be attributed to local scatterers completely surrounding the mobile receiver. This arises naturally due to the fact that the mobile array is at the same height as these local scatterers. The distance between the transmitter and receiver of approximately 1080m gives rise to an arrival time of roughly 3.6μs for the first path and is evident here. Subsequent components in the direction of increasing delay within this region are separated in the order of approximately 50ns. Intuitively, this corresponds to a local scattering disk radius of the order of 15m, which is consistent with the dimension of the width of the street where the measurement was collected.

Although limitations in resolution prevent a more detailed view of the propagation within this local scattering disk, it can be seen that within this delay region, up to four consecutive components can be identified with decreasing power as delay increases. This is possibly an effect of multiple bounce within the local scattering disk before the power is attenuated to below the 25dB cut-off.

Looking at the 0° orientation of the plot, components scattered across the delay can be identified. This corresponds to the various propagation mechanisms in the environment. Note that 0° corresponds to the direction of travel of the mobile vehicle. Figure 3 shows the equivalent plot as seen from the 2.1GHz channel at the same time. Although the exact parameters of the MPC's are different between the two channels, this is an effect of the limitation of resolution in the time and space dimension. Nonetheless, it can be appreciated that the general trend of the propagation behavior between them are similar. The path loss is approximately 1dB greater in the 2.1GHz channel as is expected when compared to the 1.9GHz channel.

B. Comparison of the Duplex Channels

The RMS Delay Spread (DS) and Azimuth Spread (AS) for the channels were calculated as the second central moment of the respective parameters. In an effort to evaluate the two duplex channels, a scatter plot of the RMS DS in the two channels is shown in Figure 4. Here, it can be seen that the two channels exhibit similar second order statistical behavior in the delay domain, with a correlation coefficient of 0.9. However, it is interesting to note that two clusters are visible in this plot. The first occurring at DS up to around 1μs and the other at DS greater than 2μs. This is possibly an indication of the kind of propagation mechanisms present in an urban environment, consisting of local scatterers which give rise to low DS, and far scatterers with paths of significant power that lead to the higher DS. This is in agreement to the COST259 Directional Channel Model [11].

Figure 5 shows the equivalent scatter plot for AS in the two channels. The evaluation of AS was less straight forward due to the wrap-around ambiguity of the azimuth parameters. This effect varies according to the assignment of the 0° boresight. Since we adopted the convention $\pm$180°, ambiguities in the AS figures arise when components are located across the $\pm$180° border.

For example, if two significant components were located at +170° and -170°, the spread of angle between them would be 340° using the above mentioned convention when the spread of angle should be 20°. This gives rise to an unrealistically large AS figure. To eliminate this possibility, the AS was evaluated with different boresight orientations by rotating it from -180° to +180°. The lowest AS figure obtained is then selected as the correct AS.

As is shown in the previous scatter plot, the two channels show a strong degree of correlation in the sense of second order statistics of the MPC's. In this case, the correlation coefficient is 0.6.

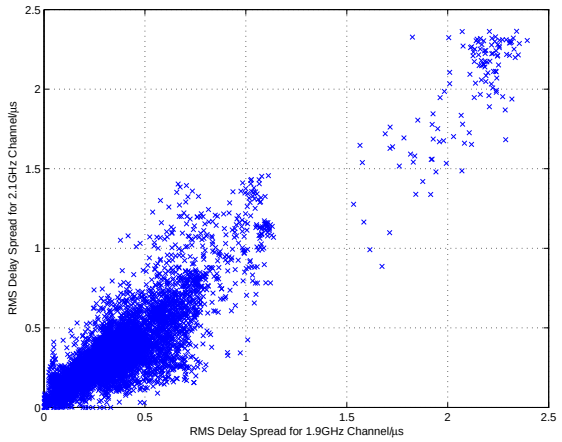

Fig. 4. Scatter Plot of RMS Delay Spread for 1.9GHz and 2.1GHz Channels

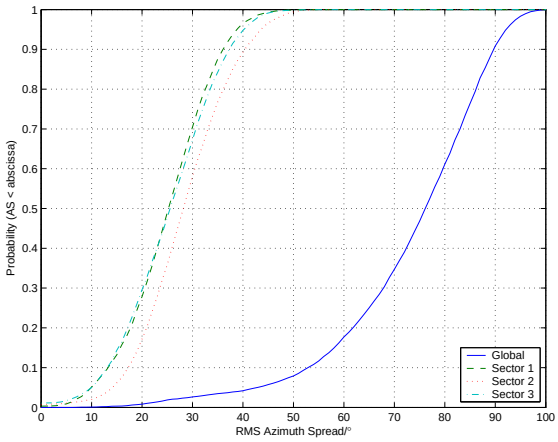

Fig. 6. CDF of RMS Azimuth Spread

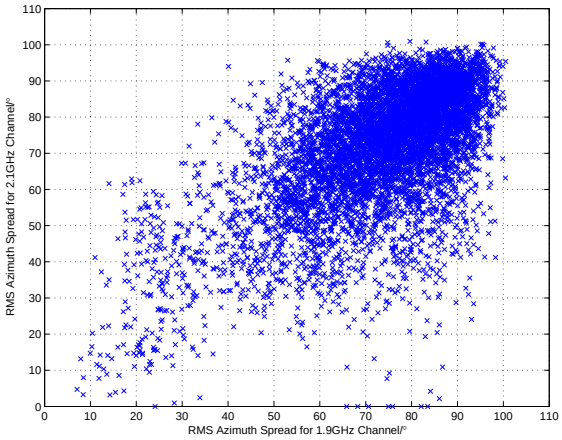

Fig. 5. Scatter Plot of RMS Azimuth Spread for 1.9GHz and 2.1GHz Channels

We can therefore conclude that since the two channels are correlated in terms of the second order statistics of the delay and azimuth parameters of the MPC's, observation of one does not lead to a significant net gain of information from the other. As such, in the next section, we shall only concentrate on the analysis of the 1.9GHz channel for the sake of clarity.

C. Distribution of the Azimuth and Delay Spreads

The CDF of the RMS AS is shown in Figure 6. Since the UCPA offers a full azimuthal view of the mobile terminal's channel, we plot the global AS as labelled in the plot. The mean value obtained here is 73.5°, which is much higher than those obtained from measurements at the base station [1].

This is a direct consequence of a low antenna height and close proximity of local scatterers that surround it completely. However, it is arguable that most mobile terminal will not employ such array architectures and thus will have a much more limited view of the channel in the azimuth plane. Therefore, we divide the global view of 360° into three equivalent sectors, each of an azimuth range of 120°. This is a more likely view of the channel as seen by multi antenna device in a practical application. Sector 1 corresponds to the azimuth range of -180° to -60° where 0° is the direction of travel. The azimuthal degrees goes in increasing order according to clockwise direction when viewed from the top of the mobile user. Similarly, Sector 2 spans -60° to +60° and finally Sector 3 covers +60° to +180°.

As a direct consequence, the RMS AS decreases to a mean of 25.5°, 29.0° and 26.0° for Sector 1, 2 and 3 respectively. This is expected since each sector sees much less of the total impinging waves from the different directions. However, the CDF indicates that the statistical distribution of the RMS AS of all three sectors are similar. When the statistics were re-evaluated where sector 1 points towards the base station, and sector 2 and 3 adjusted accordingly, we found no difference in the distribution of the statistics. This implies that that the typical RMS AS likely to be seen by a mobile terminal is independent of the direction it is facing, and thus the direction of the base station is insignificant in this respect. Moreover, in this instance, the mean RMS AS is roughly that of the global value divided by 3, thus illustrating the uniformity in azimuth of the spread of multipath components with significant energy.

Next, we present the CDF of the RMS DS in Figure 7. The mean values for the global, sector 1, 2 and 3 are 0.4μs, 0.3μs, 0.3μs and 0.3μs respectively. It can be seen that the DS varies insignificantly in this case with a narrower sector since the DS statistics are relatively evenly distributed across the azimuth plane.

Finally, to evaluate the correlation between the RMS AS and RMS DS, Figure 8 shows the scatter plot of the two parameters. Whilst in typical base station measurements, the AS and DS are well correlated [1], this situation is not evident at the mobile terminal. Here, it is obvious that AS figures are far higher and more widely spread than DS figures. This again confirms the local scatterer effect which gives rise to MPC's arriving over large azimuthal values but all with relatively similar time delays, typical of a local scattering disk. Consequently, the correlation figure was evaluated at a low 0.3 for the 1.9GHz channel and 0.2 for the 2.1GHz channel.

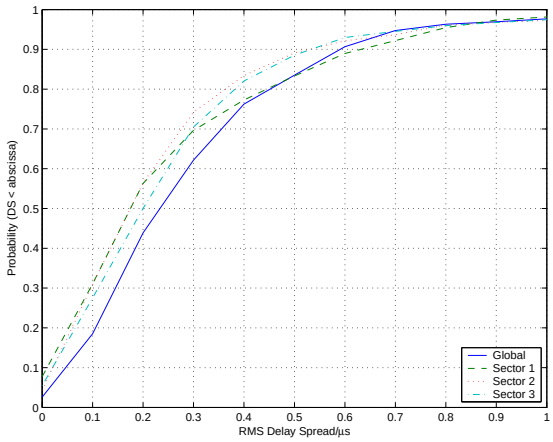

Fig. 7. CDF of RMS Delay Spread

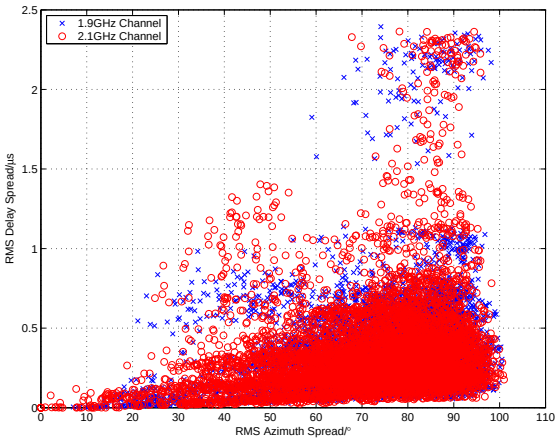

Fig. 8. Scatter Plot of RMS Delay Spread and RMS Azimuth Spread

V. Conclusions

An investigation into the properties of the MPC's as seen at the mobile terminal has been performed at the duplex bands of UTRA FDD. It has been shown that both channels exhibit similar trends in the RMS AS and DS statistics. A direct comparison of the instantaneous MPC's obtained in both channels showed that whilst the path coefficients are uncorrelated, the direction of arrival and time of arrival of MPC's are similar within the limits of resolution offered by the measurement hardware. Therefore, it is often the perception we obtain of these channels that draws to the conclusion of complete decorrelation. This is a natural effect of superposition of multiple paths that are separated outside the resolution limits of the equipment and algorithm. However, the multipath parameters such as number of paths, time of arrival, direction of arrival, direction of departure etc. are identical. The path coefficients will be of different phases since this is random.

A closer inspection of the distributions of the RMS AS shows that the figures obtained are much higher than at the base station. This is due to the effect of local scatterers at the mobile terminal. Furthermore, the RMS AS varies insignificantly with different orientations of the mobile terminal. In order words, there is no preferable directions for the mobile terminal with regards to RMS AS.

The RMS DS on the other hand is much smaller in comparison to the RMS AS. Again, this is a consequence of a local scattering disk around the mobile terminal where MPC's of significant energy arrive with very similar time delays uniformly across the azimuth range. There is a second contribution to the RMS DS from far scatterers but this effect is comparatively less dominant to the local scatterers.

Propagation mechanisms such as local scattering, street canyon coupling and rooftop diffraction were all observed. Whilst they do not always occur simultaneously, often the propagation mechanism is a combination of them.

Due to the abundance of local scattering, it is desirable to have mobile terminals that are able to sense the full azimuth plane in order to maximize the capture of energy. The requirement for temporal processing is such that multiple time delayed signals that are very closely separated but not spanned over a long delay can be resolved.

VI. Acknowledgment

The authors are grateful to the funding support of HEFCE JREI'98 for the procurement of the Medav RUSK BRI channel sounder. S. E. Foo is grateful to the University of Bristol and the UK ORS for funding towards his PhD.

References

[1] K. I. Pedersen, P. E. Mogensen and B. H. Fleury, *A Stochastic Model of the Temporal and Azimuthal Dispersion Seen at the Base Station in Outdoor Propagation Environments* IEEE Trans. VT, Vol. 49, No. 2, March 2000, pp. 437–447.

[2] R. M. Buehrer, S. Arunachalam, K. H. Wu and A. Tonello, *Spatial Channel Model and Measurements for IMT-2000 Systems* IEEE VTC, Greece, 6–9 May 2001.

[3] S. E. Foo, M. A. Beach, P. Karlsson, P. Eneroth, B. Lindmark and J. Johansson, *Spatio-Temporal Investigation of UTRA FDD Channels.* Proc. IEE 3G Mobile Communication Technologies 2002, pp. 175–179.

[4] T. Asté, P. Forster, L. Féty and S. Mayrargue, *Downlink Beamforming Avoiding DOA Estimateion for Cellular Mobile Communications* IEEE ICASSP, Washington, 12–15 May 1998.

[5] J. H. Winters, *Smart Antennas for Wireless Systems* IEEE Personal Communications, February 1998.

[6] C. M. Tan, P. Fletcher, M. A. Beach, A. R. Nix, M. Landmann and R. S. Thom'a *On the Application of Circular Arrays in Direction Finding Part I: Investigation into the Estimation Algorithms* 1st Annual COST 273 Workshop, Espoo, Finland, 29–30 May 2002.

[7] C. M. Tan, M. A. Beach, A. R. Nix, *Multi-dimensional DFT Beamspace SAGE Super-resolution Algorithm* IEEE SAM Workshop, Washington, 4–6 August 2002.

[8] R. S. Thomä, D. Hampicke, A. Richter, G. Sommerkorn, A. Scneider, U. Trautwein and W. Wirnitzer *Identification of Time-Variant Directional Mobile Radio Channels* IEEE Trans. Inst. and Meas., Vol. 49, pp.357–364.

[9] D. L. Paul, I. J. Craddock, C. J. Railton, P. N. Fletcher, M. Dean, *FDTD analysis and design of Probe-fed Dual-polarised Circular Stacked Patch Antenna* Microwave and Optical Tech. Letters, vol. 29, May 2001, pp. 223–226.

[10] B. H. Fleury, M. Tschudin, R. Heddergott, D. Dahlhaus and K. I. Pedersen *Channel Parameter Estimation in Mobile Radio Environments using the SAGE Algorithm* IEEE JSAC, vol. 17, No. 3, March 1999, pp. 434–449.

[11] H. Asplund, A. F. Molisch, M. Steinbauer and N. B. Mehta *Clustering of scatterers in mobile radio channels - Evaluation and modeling in the COST259 Directional Channel Model* IEEE ICC, New York, 28 April–2 May 2002.